Body sensor network-based strapdown orientation estimation: Application to human locomotion

Berno J.E. Misgeld[1], Daniel Rüschen[1], Saim Kim[2] and Steffen Leonhardt[1]

Abstract— **In this contribution, inertial and magnetic sensors are considered for real-time strapdown orientation tracking of human limb or robotic segment orientation. By using body sensor network integrated triaxial gyrometer, accelerometer, and magnetometer measurements, two orientation estimation filters are presented and subsequently designed for bias insensitive tracking of human gait. Both filters use quaternions for rotation representation, where preprocessing accelerometer and magnetometer data is conducted with the quaternion based estimation algorithm (QUEST) as a reference filter input. This results in a significant reduction of the complexity and calculation cost on the body sensor network. QUEST-based preprocessed attitude data is used for the designed extended Kalman filter (EKF) and a new complementary sliding mode observer. EKF-QUEST and complementary sliding mode observer are designed and tested in simulations and subsequently validated with a reference motion tracking system in treadmill tests.**

I. Introduction

Most recently, the results of the National Science Foundation - World Technology Evaluation Center (NSF-WTEC) European study emphasise the fundamental need for wearable miniaturised systems that enable the monitoring of for example motor activity in order to automate and quantify home rehabilitation [1]. The use of a wireless body sensor network enables scalable and easy wearable sensor systems and therefore is a key solution with possible application to different scenarios. Besides personal home care use, a rehabilitation robotics scenario is one of the promising areas to apply wireless body sensor networks, introducing inertial/magnetic sensor technologies. Miniaturised inertial/magnetic sensors are a relatively new technology, based on micro-electro-mechanical systems (MEMS). These sensors can be used to provide a low-cost, low-energy solution to orientation determination, while at the same time guaranteeing good quality of estimation. Inertial/magnetic sensors were successfully applied to attitude determination problems in a range of areas, with applications in motion capture, rehabilitation, and biomedical engineering. Considering rehabilitation engineering, for example [2] employs a three-degrees-of-freedom (DOF) gyroscope and a 3DOF accelerometer to detect gait characteristics for optimisation of drop-foot stimulation. A similar approach using inertial 6DOF sensors for orientation estimation in gait detection of stroke patients is reported by [3]. Based on the solution of the gait phase detection algorithm, a closed-loop control strategy for functional electrical stimulation (FES) was successfully implemented in simulations and experiments. Amongst other applications are for example the application of biomechatronic tools to measure and early diagnose the development of neurological disorders [4] or the human back movement estimation in patients with back pain [5].

Essentially two problems arise in attitude determination problems with inertial or inertial/magnetic sensors. On the one hand, a problem fundamental in attitude determination and navigation using inertial systems is the offset on the sensors, leading to drift when sensor outputs are integrated over time [6]. On the other hand, and a special case for rehabilitation applications, the body attached system of the strap-down sensors may move over time relative to the segment, depending for example on the strain applied to the sensor system. While the problem of sensor drift is addressed in this contribution, solutions for the displacement of strap-down sensor systems can be solved by the introduction of a body sensor network and kinematic joint constraints [7].

The problem of attitude determination with inertial/magnetic MEMS sensors was successfully addressed by different research groups, in recent years. [8] describes a portable orientation estimation device with a wireless network that uses measured gravity and geomagnetic field data with Sigma-Point Kalman Filters. The stability of the orientation estimation is thereby guaranteed in an accelerated environment. Other research groups propose extended Kalman Filter (EKF) techniques to fuse inertial/magnetic sensor data with quaternion rotation representation. A full EKF including bias-estimation is presented by [9] and a full as well as a reduced EKF based on the quaternion estimation algorithm (QUEST), using accelerometer and magnetometer vector observations is described by [10]. Both algorithms were tested using real-time experiments showing good performance. A quaternion-based complementary sliding mode observer (CSMO) is described by [11], which uses a multiplicative quaternion correction technique and a Levenberg-Marquardt algorithm to preprocess acceleration and magnetometer vector observations as an optimal attitude estimation problem. The algorithm is robust and shows promising results when tested in a bio-logging application to track animal movement. In this contribution, two filters for a 9DOF inertial/magnetic sensor module are developed for BSN-based strap-down orientation estimation in human movement. The Integrated Posture and Activity NEtwork by Medit Aachen (IPANEMA) is a BSN of modular structure and allows for easy integration of sensor modules [12]. To keep the real-time processing calculation cost low, two filters are designed and tested in simulations and with experimental data of treadmill walking.

[1] B. Misgeld, Daniel Rüschen, and S. Leonhardt are with the Philips Chair of Medical Information Technology, RWTH Aachen University, Aachen, Germany

[2] Saim Kim is with MELAG Medizintechnik oHG, Berlin, Germany

978-1-4673-6024-1/13/$31.00 ©2013 IEEE

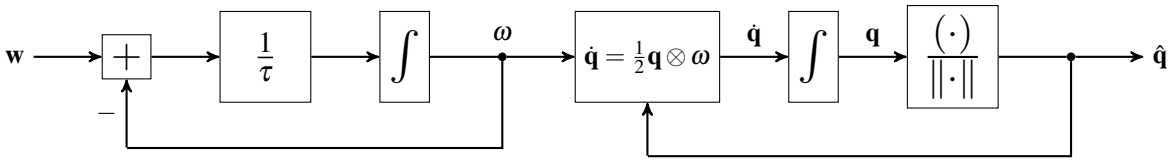

Fig. 1. Process model for the extended Kalman filter.

An extended Kalman Filter with quaternions for rotation representation and the QUEST algorithm to calculate a reference from vector observations is implemented. As an alternative approach, a modified complementary sliding mode observer including the QUEST algorithm is designed as a novel observer for robust orientation estimation. Both observers operate on a reduced set of quaternion-based equations therefore minimising the calculation cost on the BSN.
This paper is organised as follows. Chapter II describes the system of human motion used for filter design. The design of EKF-QUEST and CSMO are detailed in Chapter III, followed by a description of the BSN and the experimental setup in Chapter IV. Simulation and experimental results are given in Chapter V. Finally, conclusions are drawn and discussed in Chapter VI.

II. System Model

The process is modelled with certain assumptions about angular velocity, linear acceleration and magnetic field sensors and the dynamics of the body motion undergoing normal gait. For measured, biased, and misaligned sensor signals angular velocity $\tilde{\omega}$, linear acceleration $\tilde{\mathbf{a}}$ and magnetic field strength $\tilde{\mathbf{m}}$ given by

$$\begin{aligned}\tilde{\omega} &= \mathbf{K}_\omega \omega^n + \mathbf{b}_\omega + \mathbf{v}_\omega \\ \tilde{\mathbf{a}} &= \mathbf{K}_a \left[\mathbf{C}_n^b(\mathbf{q})\left(\mathbf{g}^n + \mathbf{b}_a + \mathbf{a}^n\right)\right] + \mathbf{v}_a \\ \tilde{\mathbf{m}} &= \mathbf{K}_m \mathbf{C}_n^b(\mathbf{q})\mathbf{h}^n + \mathbf{b}_m + \mathbf{v}_m,\end{aligned} \tag{1}$$

where $\omega^n, \mathbf{a}^n, \mathbf{m}^n$ are the truth angular rate, linear acceleration and magnetic field strength, $\mathbf{b}_\omega, \mathbf{b}_a, \mathbf{b}_m$ are bias vectors, $\mathbf{K}_\omega, \mathbf{K}_a, \mathbf{K}_m$ account for scale factors and misalignment, $\mathbf{C}_n^b$ is the transformation matrix from inertial (navigation) to body frame, $\mathbf{g}^n$ is the gravity vector and $\mathbf{v}_\omega, \mathbf{v}_a, \mathbf{v}_m$ are sensor white noise processes, for which is assumed

$$E\left[\mathbf{v}(t)\right] = \mathbf{0} \quad E\left[\mathbf{v}(t)\mathbf{v}^T(t-\tau)\right] = \mathbf{R}(t)\delta(t-\tau). \tag{2}$$

The process model for the extended Kalman filter follows the idea that a certain frequency content is inherent to limb movement and therefore orientation in normal walking. The process model is given in Figure 1 and was adapted from [10]. A first-order dynamics (low-pass) with time constant τ corresponding to the bandwidth of limb movement, driven by white noise $\mathbf{w}$. The state-space equations including quaternion rotation dynamics are given by

$$\begin{aligned}\begin{bmatrix}\dot{\omega}_1 \\ \dot{\omega}_2 \\ \dot{\omega}_3\end{bmatrix} &= \begin{bmatrix}\dot{x}_1 \\ \dot{x}_2 \\ \dot{x}_3\end{bmatrix} = \frac{1}{\tau}\left(-\begin{bmatrix}x_1 \\ x_2 \\ x_3\end{bmatrix} + \begin{bmatrix}w_1 \\ w_2 \\ w_3\end{bmatrix}\right) \\ \begin{bmatrix}\dot{q}_1 \\ \dot{q}_2 \\ \dot{q}_3 \\ \dot{q}_4\end{bmatrix} &= \begin{bmatrix}\dot{x}_4 \\ \dot{x}_5 \\ \dot{x}_6 \\ \dot{x}_7\end{bmatrix} = \frac{1}{2}\begin{bmatrix}x_4 \\ x_5 \\ x_6 \\ x_7\end{bmatrix} \otimes \begin{bmatrix}0 \\ x_1 \\ x_2 \\ x_3\end{bmatrix},\end{aligned} \tag{3}$$

with $\otimes$ denoting the quaternion multiplication. With the introduction of the short form and the measurement equation the resulting nonlinear state-space model is given by

$$\begin{aligned}\frac{d\mathbf{x}}{dt} &= \mathbf{f}(\mathbf{x}) + \mathbf{B}\mathbf{w}(t) \\ \mathbf{z} &= \mathbf{x} + \mathbf{v},\end{aligned} \tag{4}$$

where $\mathbf{x} \in \mathbb{R}^7$, $\mathbf{w} \in \mathbb{R}^3$ and $\mathbf{z} = \left[\omega^T, \mathbf{q}^T\right]^T \in \mathbb{R}^7$ being the bias, scale factor and misalignment corrected measurement vector (1) in case of ω without noise $\mathbf{v}_\omega$. Note that the noise vector applied to the quaternion vector $\mathbf{v}^T = [\mathbf{v}_\omega^T\ \mathbf{v}_\mathbf{q}^T]$ is due to the propagated sensor noise from QUEST.
For the complementary sliding mode observer the nonlinear state-space model of (4) is rearranged to the following form

$$\begin{aligned}\frac{d\mathbf{x}}{dt} &= \mathbf{f}(\hat{\mathbf{x}}) + \mathbf{B}\mathbf{w}(t) \\ \mathbf{y} &= \mathbf{g}(\mathbf{x}) + \mathbf{v},\end{aligned} \tag{5}$$

with the nonlinear state-equation being equivalent to (4), except for $\hat{\mathbf{x}} = \left[\omega^T \quad \frac{\mathbf{q}^T}{\|\mathbf{q}\|_2}\right]^T$. The system output equation of (5) can thereby be rewritten as

$$\mathbf{y} = \begin{bmatrix}\omega \\ \hat{\mathbf{q}}\end{bmatrix} + \mathbf{v} = \left[\omega^T \quad \frac{\mathbf{q}^T}{\|\mathbf{q}\|_2}\right]^T + \mathbf{v}. \tag{6}$$

III. Filter Design

A. Quaternion estimation algorithm (QUEST)

Since two body-fixed vector observations are available at a single time, it is possible to solve the problem of determining the attitude in the inertial or reference frame. This is usually referred to as Wahba's problem, which is to find the orthogonal matrix $\mathbf{C}$ with determinant +1 (rotation matrix) that minimises the loss function [13]

$$L(\mathbf{C}) = \frac{1}{2}\sum_i a_i \left|\mathbf{b}_i - \mathbf{C}\mathbf{r}_i\right|^2 \tag{7}$$

where a_i are nonnegative weights, $\mathbf{b}_i$ are body-fixed frame unit vector observations, and $\mathbf{r}_i$ are corresponding unit vectors in the inertial frame. Eq. (7) can be rearranged to

$$L(\mathbf{C}) = \sum_i a_i - \mathrm{tr}(\mathbf{C}\mathbf{B}^{\mathrm{T}}) \tag{8}$$

with

$$\mathbf{B} = \sum_i a_i \mathbf{b}_i \mathbf{r}_i^{\mathrm{T}}. \tag{9}$$

With the assumption of a unit quaternion and subsequent parametrisation of the attitude matrix [13], it follows with

$$\mathrm{tr}(\mathbf{C}\mathbf{B}^{\mathrm{T}}) = \mathbf{q}^T \mathbf{K} \mathbf{q}, \tag{10}$$

which is to be maximised in order to minimise (8), where

$$\mathbf{K} = \begin{bmatrix} \mathrm{tr}(\mathbf{B}) & \mathbf{z}^{\mathrm{T}} \\ \mathbf{z} & \mathbf{S} - \mathrm{tr}(\mathbf{B})\mathbf{I}_3 \end{bmatrix} \tag{11}$$

with

$$\mathbf{S} = \mathbf{B} + \mathbf{B}^{\mathrm{T}}, \quad \mathbf{z} = \begin{bmatrix} b_{23} - b_{32} \\ b_{31} - b_{13} \\ b_{12} - b_{21} \end{bmatrix}. \tag{12}$$

Maximising (10) leads to the optimal attitude estimation and is clearly achieved by finding the maximum eigenvalue $\bar{\lambda}(\mathbf{K})$ with the corresponding optimal quaternion according to the eigenvalue problem

$$\mathbf{K}\mathbf{q}_{opt} = \bar{\lambda}\mathbf{q}_{opt}. \tag{13}$$

Partitioning and rearranging of (13) according to the optimal unit quaternion

$$\mathbf{q}_{\mathrm{opt}} = \frac{1}{\sqrt{\hat{q}_1^2 + \|\hat{\mathbf{e}}\|^2}} \begin{bmatrix} \hat{q}_1 \\ \hat{\mathbf{e}} \end{bmatrix} \tag{14}$$

leads to

$$\begin{aligned} \hat{q}_1 &= \alpha\,(\lambda_{\max} + \mathrm{tr}(\mathbf{B})) - \det(\mathbf{S}) \\ \hat{\mathbf{e}} &= \left(\alpha\mathbf{I}_{3\times 3} + (\lambda_{\max} - \mathrm{tr}(\mathbf{B}))\mathbf{S} + \mathbf{S}^2\right)\mathbf{z} \end{aligned} \tag{15}$$

with

$$\alpha = \bar{\lambda}^2 - (\mathrm{tr}(\mathbf{B}))^2 + \mathrm{tr}(\mathrm{adj}(\mathbf{S})) \tag{16}$$

and concludes the quaternion estimation algorithm.

B. Extended Kalman Filter with QUEST

The extended Kalman filter uses a first-order Taylor approximated linearisation of the nonlinear process model (4)

$$\frac{d\Delta\mathbf{x}}{dt} = \left.\frac{\partial \mathbf{f}(\mathbf{x})}{\partial \mathbf{x}}\right|_{\mathbf{x}=\hat{\mathbf{x}}} \Delta\mathbf{x} + \mathbf{B}\mathbf{w}, \tag{17}$$

where $\Delta\mathbf{x} = \mathbf{x} - \hat{\mathbf{x}}$. Since measurement data is sampled at equidistant time intervals Δt, the corresponding linearised difference equation is given by

$$\Delta\mathbf{x}_{k+1} = \Phi_k \Delta\mathbf{x}_k + \mathbf{B}_k\mathbf{w}_k, \tag{18}$$

with sampling instances k and the discrete state-transition matrix Φ_k, which is derived from the matrix exponential

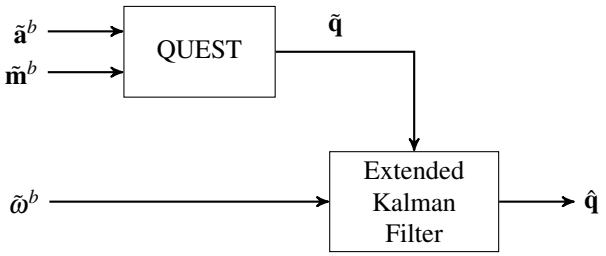

Fig. 2. Block diagram of the extended Kalman filter with the quaternion estimation algorithm (QUEST).

$e^{\mathbf{A}\Delta t} \approx \mathbf{I}_7 + \mathbf{A}\Delta t$, neglecting terms of higher order in the lower 4×7-part of the matrix

$$\Phi_k = \begin{bmatrix} e^{\frac{-\Delta t}{\tau_1}} & 0 & 0 & 0 & 0 & 0 & 0 \\ 0 & e^{\frac{-\Delta t}{\tau_2}} & 0 & 0 & 0 & 0 & 0 \\ 0 & 0 & e^{\frac{-\Delta t}{\tau_3}} & 0 & 0 & 0 & 0 \\ \frac{-\hat{x}_5\Delta t}{2} & \frac{-\hat{x}_6\Delta t}{2} & \frac{-\hat{x}_7\Delta t}{2} & 1 & \frac{-\hat{x}_1\Delta t}{2} & \frac{-\hat{x}_2\Delta t}{2} & \frac{-\hat{x}_3\Delta t}{2} \\ \frac{\hat{x}_4\Delta t}{2} & \frac{\hat{x}_7\Delta t}{2} & \frac{-\hat{x}_6\Delta t}{2} & \frac{\hat{x}_1\Delta t}{2} & 1 & \frac{-\hat{x}_3\Delta t}{2} & \frac{\hat{x}_2\Delta t}{2} \\ \frac{-\hat{x}_7\Delta t}{2} & \frac{\hat{x}_4\Delta t}{2} & \frac{\hat{x}_5\Delta t}{2} & \frac{\hat{x}_2\Delta t}{2} & \frac{\hat{x}_3\Delta t}{2} & 1 & \frac{-\hat{x}_1\Delta t}{2} \\ \frac{\hat{x}_6\Delta t}{2} & \frac{-\hat{x}_5\Delta t}{2} & \frac{\hat{x}_4\Delta t}{2} & \frac{\hat{x}_3\Delta t}{2} & \frac{-\hat{x}_2\Delta t}{2} & \frac{\hat{x}_1\Delta t}{2} & 1 \end{bmatrix}. \tag{19}$$

The discretised measurement model for the EKF is given by

$$\mathbf{z}_k = \mathbf{x}_k + \mathbf{v}_k, \tag{20}$$

in which in a similar way to (4) the discrete noise process entries corresponding to quaternions are accelerometer and magnetometer measurement noise propagated through the QUEST. Covariance matrices for process and measurement noise are $\mathbf{Q}_k = \mathrm{E}\left[\mathbf{w}_k\mathbf{w}_k^{\mathrm{T}}\right]$ and $\mathbf{R}_k = \mathrm{E}\left[\mathbf{v}_k\mathbf{v}_k^{\mathrm{T}}\right]$. The standard equations of the time-varying extended Kalman filter are implemented [10], where the QUEST reference quaternion vector and measured angular rates are used as the measurement vector (20). Figure 2 shows a block diagram of the EKF-QUEST structure.

C. Complementary sliding mode observer

The complementary sliding mode observer is based on the process model given in equation (6), for which the output is rewritten as

$$\hat{\mathbf{q}} = \begin{bmatrix} \omega \\ \hat{\mathbf{q}} \end{bmatrix} + \mathbf{v} = \begin{bmatrix} \omega^T & \dfrac{[q_1\ q_2\ q_3\ q_4]}{\sqrt{q_1^2 + q_2^2 + q_3^2 + q_4^2}} \end{bmatrix}^T + \mathbf{v}. \tag{21}$$

The linearised system at the operating point $\bar{\mathbf{q}}$, $\bar{\omega}$ can be obtained from (21) with $\Delta\mathbf{q} = \hat{\mathbf{q}} - \bar{\mathbf{q}}$ and $\Delta\omega = \hat{\omega} - \bar{\omega}$ with $\Delta\mathbf{x}^T = [\Delta\omega^T\ \Delta\mathbf{q}^T]$ as

$$\begin{aligned} \frac{d\Delta\mathbf{x}}{dt} &\approx \left.\frac{\partial \mathbf{f}(\hat{\mathbf{x}})}{\partial \hat{\mathbf{x}}}\right|_{\hat{\mathbf{x}}=\bar{\mathbf{x}}} \Delta\mathbf{x} + \mathbf{B}\mathbf{w} \\ \Delta\hat{\mathbf{y}} &\approx \left.\frac{\partial \mathbf{g}(\hat{\mathbf{x}})}{\partial \hat{\mathbf{x}}}\right|_{\hat{\mathbf{x}}=\bar{\mathbf{x}}} \Delta\mathbf{x} + \mathbf{v}. \end{aligned} \tag{22}$$

Note that for the partial derivatives of higher order than one are neglected in the Taylor-approximation and that the output equations are limited to first-order derivatives. In addition,

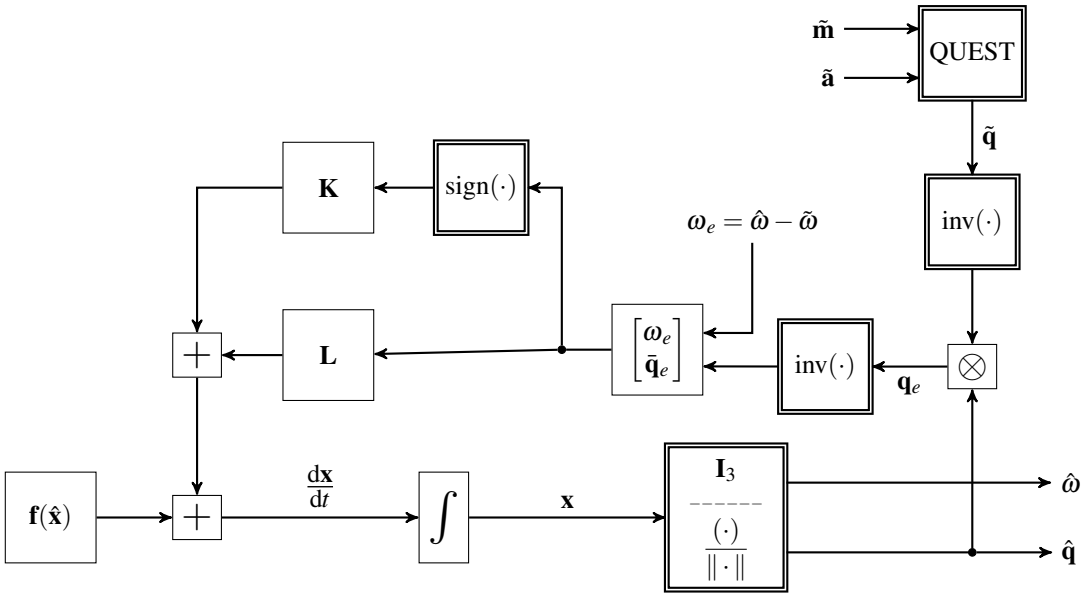

Fig. 3. Block diagram of the complementary sliding mode observer with QUEST.

the 2-norm quaternion normalisation has to be regarded in the state-linearisation. The lower-right block of the resulting linearised system matrix is skew-symmetric in $\mathbf{A}_{CSMO} \in \mathbb{R}^{4\times4}$, which means that the eigenvalues always come in imaginary-axis pairs. This corresponds to the critically stable case and a continuous rotation for non-zero angular rates. The proposed sliding mode observer block-diagram is shown in Figure 3. The error for the measured and model rates is thereby

$$\omega_e = \hat{\omega} - \tilde{\omega}. \tag{23}$$

Considering the estimated quaternion output, calculated from (21), the orientation error between QUEST optimal orientation $\mathbf{q}_{opt}$ and $\hat{\mathbf{q}}$ is given by

$$\mathbf{q}_e = \hat{\mathbf{q}} \otimes \tilde{\mathbf{q}}^{-1}. \tag{24}$$

The estimation error quaternion is again rotated to obtain negative feedback gain error unit quaternion $\bar{\mathbf{q}}_e = \mathbf{q}_e^{-1}$. For the observer feedback measurement errors of ω_e and $\bar{\mathbf{q}}_e$ are rearranged to the error vector $\mathbf{y}_e^T = [\omega_e^T \; \bar{\mathbf{q}}_e^T]$. The complementary sliding mode observer consists of a linear Luenberger feedback gain $\mathbf{L}$ and a switching function

$$\nu = \begin{cases} \mathbf{K}\frac{\mathbf{y}_e}{\|\mathbf{y}_e\|_2} & \mathbf{y}_e \neq 0 \\ \mathbf{0} & \text{otherwise} \end{cases} \tag{25}$$

where $\mathbf{K} = \text{diag}(\mathbf{k}_\omega^T, \mathbf{k}_\mathbf{q}^T)$ is the discontinuous sliding mode observer (SMO) gain matrix with $\mathbf{k}_\omega$ the gain applied to the ω_e and $\mathbf{k}_\mathbf{q}$ applied to the $\bar{\mathbf{q}}_e$ vector. The CSMO feedback correction terms are added based on the assumption that small attitude changes occur over a sampling time interval. Therefore, the action of the CSMO on the observer model is given by

$$\begin{aligned} \frac{d\mathbf{q}}{dt} &= \nu \oplus \mathbf{L}\bar{\mathbf{y}}_e \oplus \mathbf{f}(\hat{\mathbf{x}}) \oplus \mathbf{B}\mathbf{w} \\ \hat{\mathbf{y}} &= \begin{bmatrix} \hat{\omega}^T & \frac{\mathbf{q}^T}{\|\mathbf{q}\|_2} \end{bmatrix}^T. \end{aligned} \tag{26}$$

with $\oplus$, the quaternion addition and ω, the measured and corrected angular rates. Note that the Luenberger-type observer feedback gain matrix is parametrised as $\mathbf{L} = \text{diag}(\mathbf{l}_\omega^T, \mathbf{l}_\mathbf{q}^T)$, where parameters for $\mathbf{L}$ and for $\mathbf{K}$ were determined for the linearised model in simulations and experiments in a heuristic way. Although the sliding mode observer guarantees a robust sliding motion in face of uncertainties corresponding to nonlinearities and unknown dynamics/parameter variation, the stability of the CSMO was formally not proven, but verified in simulations and experiments.

IV. Body Sensor Network and Experimental Setup

The IPANEMA body sensor network uses a 433 MHz industrial, scientific and medical (ISM) band transceiver (CC1101 Texas Instruments Inc., USA), which is less prone to electromagnetic shadowing effects by the human body, although a lower data rate can be achieved [12]. The IPANEMA BSN is able to deliver a data rate of 250 kbps which is not critical for most biomedical applications. Both hardware and software is designed in a modular way, allowing for the adaption and extension with different sensors and actuators. The IPANEMA used for the measurements is in generation 2.5 and can be easily attached to different segments of the human body. Besides the wireless transceiver, the main functional units of the BSN master and slave nodes are the microcontroller (MSP430F1611, Texas Instruments Inc., USA), the power management (LTC3558, Linear Technology, USA) and two extension ports (CLP160-02-X-D, Samtec, USA). To measure the segment orientation with the IPANEMA BSN, a 9DOF inertial/magnetic sensor

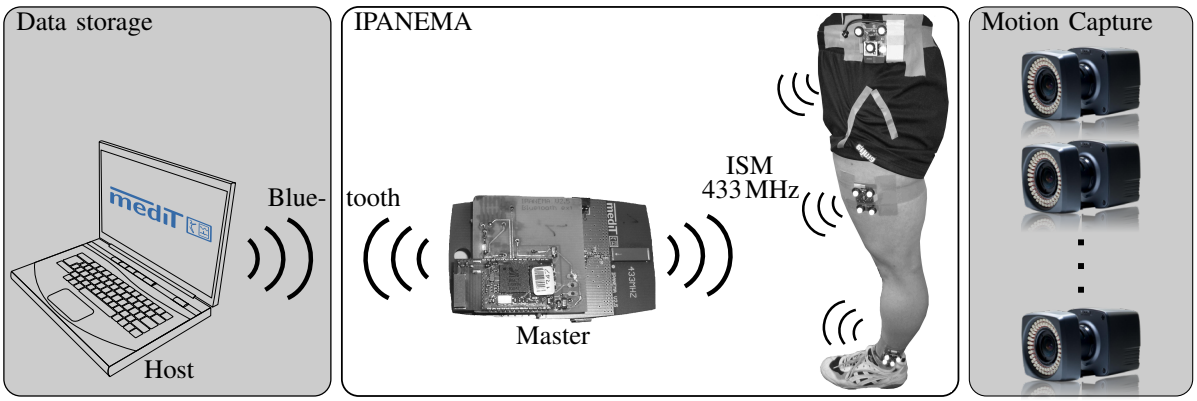

Fig. 4. Overview of the experimental setup.

board (ADIS16400, Analog Devices, USA) was designed. Mounted on the body segment, the slave BSN node sends the inertial/magnetic data to the BSN master node, which in turn is connected to a host computer for data recording.
Measurements of human locomotion were conducted on a treadmill (Ergo Run Medical 8, Daum Electronic GmbH, Germany) employing the IPANEMA BSN. The test person was fitted with three BSN nodes, mounted on foot ankle, at the thigh and at the hip. Data was recorded over 2.5 minutes of walking at different speeds (2-6 km/h). At the same time, reference trajectory data was recorded with a motion capture system with six infrared cameras (Vicon Bonita, Vicon, USA). Figure 4 shows an overview of the test setup. The six motion capture cameras track markers, attached to the BSN nodes and are connected to a host computer for recording (Vicon Software, Vicon, USA). Collected data from the BSN nodes is stored on another computer. At the start of each measurement day, random movements were recorded with each node and the reference system, to be used for sensor calibration. The sensor calibration is a two step procedure, using the motion capturing tracked BSN node in a first step at rest and in a second step under random movements.

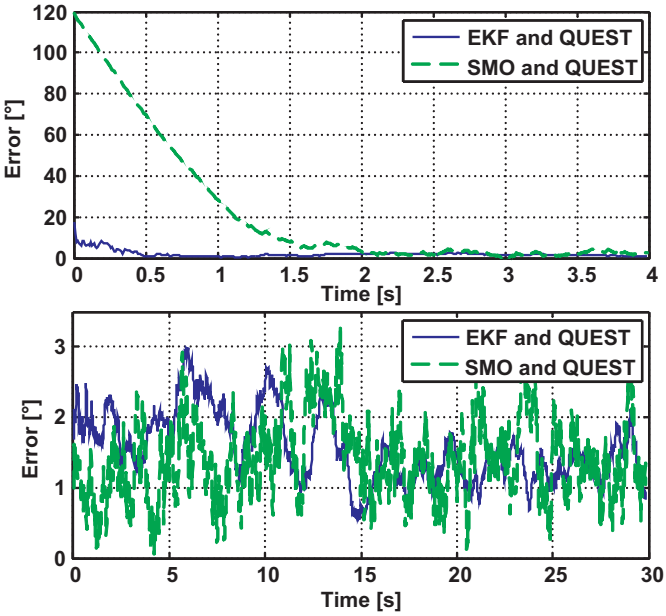

Fig. 5. EKF-QUEST and SMO filter convergence for stationary and sinusoidal tests (upper: stationary test, lower: sinusoidal movement).

V. Simulation and Experimental Results

Before conducting treadmill locomotion experiments with the real system, a simulative study was conducted to test stationary and dynamic convergence of the filter. Stationary and sinusoidal data were corrupted by noise and used as available sensor measurements in the simulations. Figure 5 shows the results of two exemplary simulations. It can be clearly seen that both filters converge fast, with the SMO having the larger initial error. The difference in the errors is due initial preference of the QUEST-solution over the initial state of the filter in the EKF-Quest algorithm and not because of a different initial state. For a sinusoidal movement in body roll direction with an amplitude of $\frac{\pi}{4}$ rad and a frequency of 2 Hz, the absolute quaternion errors of both filters remain below 2.5°. Similar results were obtained at different walking speeds with the movement taking place in different axes.
Under experimental conditions and after successful calibration of sensor data, the transformation matrices between motion tracking and BSN reference frames were obtained in a first step. Sensor data was continuously recorded with the BSN and saved on a computer at a sampling rate of 75 Hz. As an initial experiment, the BSN was tracked in stationary conditions (not moving) and the orientation was determined with the EKF-QUEST and the SMO-QUEST. Figure 6 shows the result of an experimental convergence test. It can be seen that the EKF-QUEST is converging slightly faster that the SMO-QUEST, with both filters showing a good response. Note however, that the difference in the remaining offset of 4°, is due to a remaining error between reference frames of motion tracking and BSN. The lower initial error of the QUEST-EKF is due to a preferred initial QUEST-solution over the initial state of the filter in the EKF-QUEST algorithm. Dynamic measurements of human locomotion were conducted at different walking speeds on the treadmill, while tracking the BSN. Figure 7 shows an exemplary result of the tracking with a subject walking at 3 km/h with the

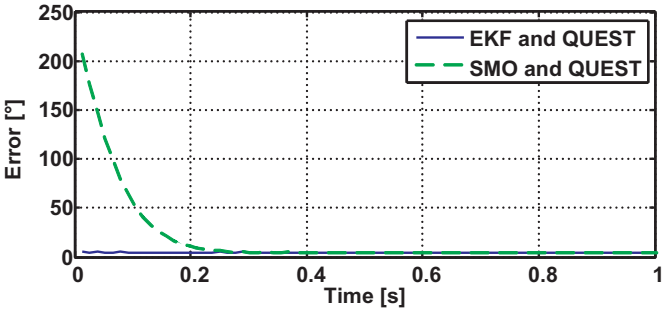

Fig. 6. EKF-QUEST and SMO filter convergence at stationary conditions.

sensor located at the hip. It can be seen that the absolute orientation error between motion tracking and BSN results in peak values of about 8° for the EKF-QUEST and 10-12° for the SMO-QUEST. The peaks can be attributed to the QUEST algorithm, where the vector observations degrade due to accelerations at foot impact. However, the root mean squared error is quite good with 5.4° for the EKF-QUEST and 8.3° for the SMO-QUEST, bearing in mind that the convergence error in stationary tests was still 4°. Tests with the system at different walking speeds lead to similar results. Both filters were stable in all of the conducted test runs (ranging from 2-6 km/h).

VI. Conclusions and Discussion

Two attitude estimation filters to be used in a strapdown BSN application were designed and tested in simulations and experiments. Both filters use quaternions as a representation for rotation between the body fixed and an inertial reference frame, leading to a reduced set of equations/complexity and the associated advantage in calculation cost on the BSN. The IPANEMA BSN with a 433 MHz ISM band was reliably employed during the tests and transmitted data of up to three 9DOF nodes (number of available nodes). The well-known extended Kalman filter was compared to a novel complementary sliding mode observer. Both filters employ the quaternion estimation algorithm. The performance of the EKF-QUEST is slightly superior to the SMO-QUEST. However, bearing in mind the exceeding complexity of the EKF-QUEST, this is a most promising result. A number of experiments were conducted at different walking speeds and at different joint positions leading to good results measured in terms of absolute and RMS errors between the BSN and a motion capturing reference system. Furthermore, the parameters of the CSMO switching and Luenberger typer observer feedback matrices were designed in a heuristic approach, with suggested suboptimal results. Therefore, future work will consider the implementation of the filters on the body sensor network processor and the systematic, adaptive design of the CSMO observer feedback matrices.

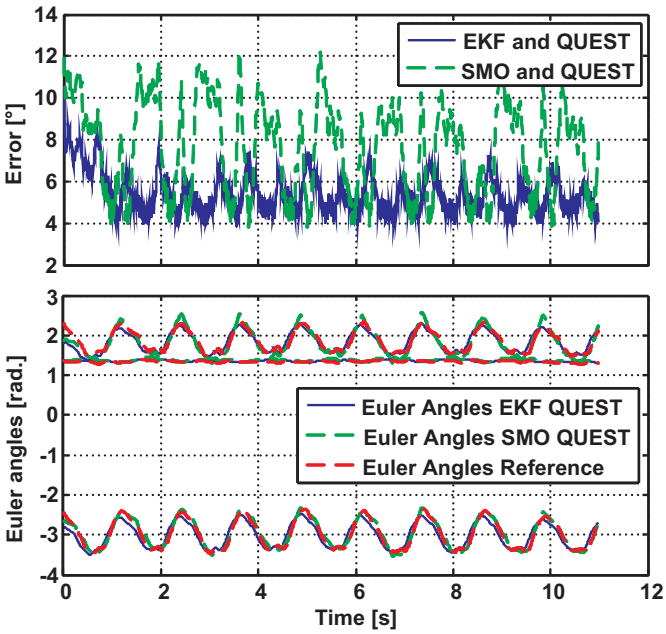

Fig. 7. EKF-QUEST and SMO-QUEST filter in a human walking experiment (upper: absolute error, lower: Euler angles).

References

[1] D. Reinkensmeyer, D. Paolo Bonato, M. Boninger, L. Chan, R. Cowan, B. Fregly, and M. Rodgers, "Major trends in mobility technology research and development: Overview of the results of the nsf-wtec european study," *Journal of NeuroEngineering and Rehabilitation*, vol. 9(22), 2012.

[2] D. Kotiadis, H. Hermens, and P. Veltink, "Inertial gait phase detection for control of a drop foot stimulator: Inertial sensing for gait phase detection," *Med. Eng. Phys.*, vol. 32(4), pp. 287–297, 2010.

[3] N.-O. Negard, "Controlled fes-assisted gait training for hemiplegic stroke patients based on inertial sensor," Ph.D. dissertation, TU Berlin, 2009.

[4] D. Campolo, M. Molteni, E. Guglielmelli, F. Keller, C. Laschi, and D. P., "Towards development of biomechatronic tools for early diagnosis of neurodevelopmental disorders," in *EMBS*. IEEE, 2006, pp. 3242–3245.

[5] Z.-Q. Zhang, J. Pansiot, B. Lo, and G.-Z. Yang, "Human back movement analysis using bsn," in *Int. Conference on Body Sensor Networks*. IEEE, 2011, pp. 13–18.

[6] J. Crassidis, F. Markley, and Y. Cheng, "A survey of nonlinear attitude estimation methods," *Journal of Guidance Control and Dynamics*, vol. 30, 2007.

[7] M. El-Gohary and J. McNames, "Shoulder and elbow joint angle tracking with inertial sensors," *Biomedical Engineering, IEEE Transactions on*, vol. 59, no. 9, pp. 2635 –2641, sept. 2012.

[8] T. Harada, H. Uchino, T. Mori, and T. Sato, "Portable absolute orientation estimation device with wireless network under accelerated situation," in *International Conference on Robotics and Automation*, vol. 2, 2004, pp. 1412–1417.

[9] A. Sabatini, "Quaternion-based extended kalman filter for determining orientation by inertial and magnetic sensing," *IEEE Transactions on Biomedical Engineering*, vol. 53, no. 7, pp. 1346–1356, 2006.

[10] X. Yun and E. Bachmann, "Design, implementation, and experimental results of a quaternion-based kalman filter for human body motion tracking," *IEEE Transactions on Robotics*, vol. 22, no. 6, pp. 1216–1227, 2006.

[11] H. Fourati, N. Manamanni, A. Jemaa, L. Afilal, and Y. Handrich, "A quaternion-based complementary sliding mode observer for attitude estimation: Application in free-ranging animal motions," in *Conference on Decision and Control*, vol. 49. IEEE, 2010, pp. 5056–5061.

[12] S. Kim, C. Brendle, H.-Y. Lee, M. Walter, S. Gloeggler, and S. Leonhardt, "Evaluation of a 433 mhz band body sensor network for biomedical applications," *Sensors*, vol. 13(1), pp. 898–917, 2013.

[13] F. Markley and D. Mortari, "Quaternion attitude estimation using vector observations," *Journal of Astronautical Sciences*, vol. 48, pp. 359–380, 2000.